

Lattice dynamics and electron-phonon coupling in transition metal diborides

R. Heid¹, B. Renker¹, H. Schober², P. Adelmann¹, D. Ernst¹, and K.-P. Bohnen¹

¹*Forschungszentrum Karlsruhe, IFP, P.O.B. 3640, D-76021 Karlsruhe, Germany and*

²*Institut Laue-Langevin, BP 156 X, F-38042 Grenoble Cedex, France*

(Dated: October 31, 2018)

The phonon density-of-states of transition metal diborides TMB₂ with TM = Ti, V, Ta, Nb and Y has been measured using the technique of inelastic neutron scattering. The experimental data are compared with ab initio density functional calculations whereby an excellent agreement is registered. The calculations thus can be used to obtain electron-phonon spectral functions within the isotropic limit. A comparison to similar data for MgB₂ and AlB₂ which were subject of prior publications as well as parameters important for the superconducting properties are part of the discussion.

PACS numbers: 74.25.kc, 63.20.kr, 78.70.Nx, 71.20.Lp

The discovery of superconductivity in MgB₂ at the unexpected high temperature of 39 K has renewed the interest in diboride compounds. The well known AlB₂ structure (*P6/mmm*) is formed with quite a number of transition metals (TM) [2]. However, a clear proof of superconductivity could not be established for any of these candidates. Obviously the influence of lattice faults on the transport properties is important. A unique feature for MgB₂ is the depopulation of B $2p - \sigma$ bands due to a particular Mg-B interaction [1]. It has been shown by band structure calculations for the TM-diborides that E_F moves up into the TM $4d$ -states with the consequence that these compounds behave more like normal metals [3]. Most important for the transport properties is the electron-phonon interaction in these systems. Very recently results from point contact spectroscopy have been reported for TM = Zr, Nb, and Ta. The authors conclude on an only modest electron-phonon interaction parameter for these samples [4]. A general investigation of the phonon spectra of TM-diborides has so far not been performed. In the present paper we confront measurements of the generalized phonon density of states for selected compounds with TM = Ta, V, Nb, Ti, and Y with ab initio density functional theory (DFT) calculations. Results for electron-phonon spectral functions are derived and placed in context to previous investigations of superconducting MgB₂.

All diborides were prepared from stoichiometric mixtures of TM elements and amorphous ¹¹B. We have chosen the less absorbing ¹¹B in view of the intended inelastic neutron scattering (INS) experiments. The mixed powders were compacted to pellets and arc melted. The final polycrystalline samples showed metallic brightness and were found to be single phase by x -ray diffraction. All of our samples failed to show superconductivity above 4 K although transition temperatures for the pure elements of Nb and Ta with 9.2 K and 4.39 K are known. Our INS experiments were performed on the IN6 time-of-flight spectrometer at the HFR in Grenoble, France, with an incident neutron energy of 4.75 meV at 300 K in the upscattering mode. A high chopper speed of 201 rms and focusing in the inelastic region was used to improve the resolution. The generalized phonon density of states

TABLE I: Structural and scattering parameters for selected diborides. Distances are given in Å. The values in brackets apply to optimized geometries found in the DFT calculations after energy optimization. M-B and B-B denote the shortest metal-boron and boron-boron distances, respectively, and m is the TM mass number. σ/m is the neutron scattering cross-section over the mass in barn/amu.

	MgB ₂	AlB ₂	TaB ₂	VB ₂	NbB ₂	TiB ₂	YB ₂
a	3.084 (3.056)	3.009 (2.965)	3.08 (3.08)	2.998 (2.979)	3.09 (3.093)	3.038 (2.998)	3.290 (3.254)
c	3.522 (3.622)	3.262 (3.232)	3.265 (3.272)	3.056 (2.995)	3.3 (3.337)	3.23 (3.188)	3.835 (3.830)
M-B	2.504	2.383	2.421	2.297	2.477	2.409	2.716
B-B	1.781	1.737	1.799	1.772	1.794	1.773	1.914
m	24.312	26.982	180.948	59.42	92.906	47.90	88.91
σ/m	0.151	0.056	0.033	0.098	0.067	0.085	0.087

(GDOS) has been calculated from the recorded intensities integrated over a scattering region from 14° to 114°. For the data evaluation we have applied multi-phonon corrections in a self-consistent procedure. The GDOS implies a weighting of vibrational modes of by σ/m (scattering cross-section over the mass, see Tab. I). For comparison the scattering power of ¹¹B is 0.525 barn/amu.

Fig. 1 shows a comparison of GDOS spectra for all investigated TM-diborides. Each spectrum is normalized to 1. The most significant common feature is a gap around 40 to 50 meV. When analyzing the respective intensities we find that the high-frequency band is essentially composed of boron vibrations. The gap is thus a consequence of the large mass difference, which leads to a decoupling of transition metal and boron vibrations. A clearly different behavior is observed for MgB₂ and AlB₂ where due to the smaller mass of the metal atoms a hybridization of metal and boron modes occurs. In the low-frequency band of the transition metal diboride spectra we observe distinct shifts which however do not simply follow a \sqrt{m} relation. This indicates that there are appreciable differences in the B-TM coupling. This conclusion is confirmed by the concomitant variations of interatomic distances (Tab. I). Somewhat more surprising is the fact that significant frequency shifts are equally registered for

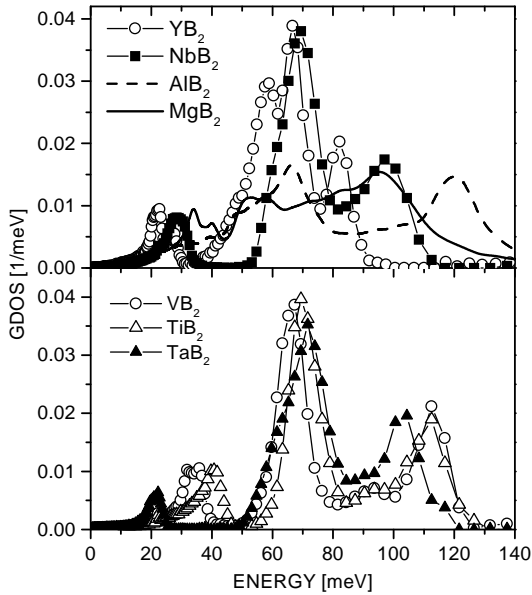


FIG. 1: The experimental generalized phonon density-of-states for various transition metal diborides. AlB_2 and superconducting MgB_2 are shown for comparison. Very significant changes are related to structural differences. Signature of strong electron-phonon coupling is the dramatic broadening of the highest energy B peak visible for MgB_2 but not for the other candidates.

the peak at the high-frequency end of the spectra where the lowest frequency is found in YB_2 . The E_{2g} and B_{1g} modes, which are important for superconductivity in MgB_2 , lie within this region where neighboring boron atoms move against each other. Strong electron-phonon coupling is expected to cause a significant broadening. This broadening is visible in the spectrum of MgB_2 but not in those of the other compounds. The low frequency of the peak in YB_2 alone can, therefore, not be taken as a signature of strong electron-phonon coupling. A simpler explanation is offered by comparatively weak B-B interactions. As can be seen from Tab. I the B-B distance is exceptionally large for this compound. If any, then the $G(\omega)$ for NbB_2 shows signatures of a stronger electron-phonon coupling, a compound for which some authors report superconductivity.

First principals density-functional calculations give parameter free insight into the electronic structure of all of these compounds. They in addition yield the lattice dynamical properties. Corresponding results are shown in Fig. 2. For the calculations we used the mixed basis pseudopotential method, which is described in some detail in Ref. [5, 6]. Norm-conserving pseudopotentials for V, Ta, Nb, Y and Ti were constructed according to the description of Bachelet-Hamann-Schlüter [7, 8], whereas for boron a Vanderbilt-type potential was created [9]. The mixed basis scheme uses a combination of local functions together with plane waves for a representation of the valence states. The good agreement between calculated and experimental structural parameters (see Tab. I) as well

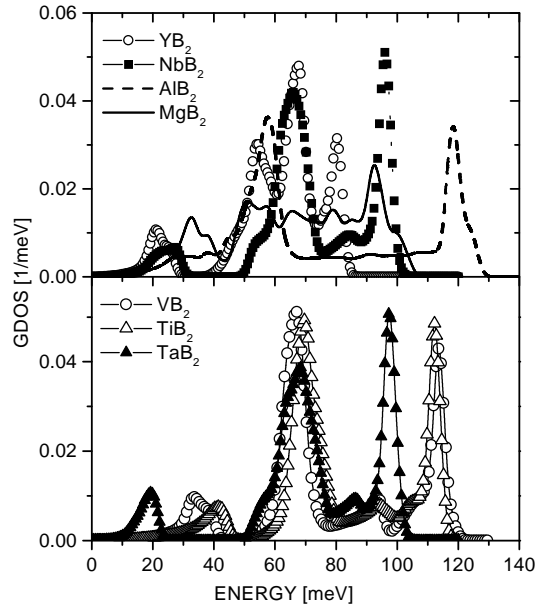


FIG. 2: Calculated GDOS spectra for all diborides shown in Fig. 1. The proper σ/m values have been applied for a direct comparison to the experimental spectra.

TABLE II: Calculated Γ point frequencies in meV.

	MgB_2	AlB_2	TaB_2	VB_2	NbB_2	TiB_2	YB_2
E_{1u}	40.5	36.6	52.6	60.6	52.0	65.5	44.1
A_{2u}	50.2	52.1	61.9	62.1	60.5	66.4	45.3
E_{2g}	70.8	125.0	100.6	114.9	98.4	112.8	75.5
B_{1g}	87.0	61.3	68.8	69.6	69.8	70.0	75.1

as between calculated and experimental phonon GDOS (Figs. 1 and 2) proves the validity of our description.

A very unique feature of electron-phonon coupling in MgB_2 is the downshift of the in-plane E_{2g} mode well below the out-of-plane B_{1g} mode. Such an inversion of the usual sequence of mode frequencies is not encountered in any of the other diborides as shown in Tab. II, where we compile the calculated Γ -point frequencies of the boron vibrations.

The present calculations prove capable of describing the lattice dynamics of various diborides with quite different electronic transport properties. For the TM diborides, the isotropic character of the d -bands has the consequence that these compounds behave electronically very much like normal 3D metals [3]. Although the band structures show strong similarities, the Fermi level E_F moves up and down within the region of the transition metal d -bands. This variable band filling leads to appreciable differences in the various interatomic distances. The E_{2g} frequencies exhibit an expected inverse correlation with the in-plane lattice constant, which indicates that the B-B covalent bond is electronically rather similar for all these compounds. On the contrast, the out-of-plane boron mode B_{1g} is very insensitive to changes in

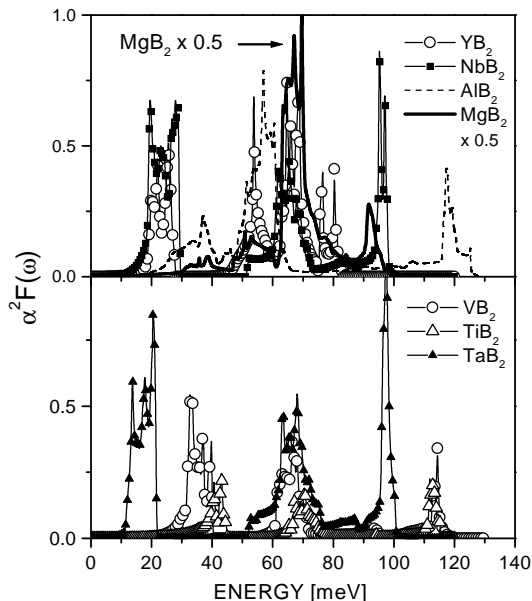


FIG. 3: Isotropic Eliashberg functions for the investigated diborides as obtained in the present calculation.

the lattice constants.

Somewhat exceptional in our series of transition metal diborides is only YB_2 . Peculiarities in the electronic structure lead to a drastic increase of both the a and c lattice constants. As a consequence of the increased B-B bond length, the longitudinal force constant of the B-B bond is strongly reduced, and becomes even smaller than the transverse coupling. This is the reason for the observed softening of the high-frequency B-modes in YB_2 .

In order to get a more quantitative picture of the electron-phonon coupling within the series of diborides we have calculated the isotropic Eliashberg function $\alpha^2 F(\omega)$ which describes the phonon mediated pairing interaction (Fig. 3). Details of the computations are outlined in Ref. [5]. Again MgB_2 proves to be singular. The extremely strong coupling at high-phonon frequencies is known to be connected to the E_{2g} boron in-plane mode. It is found as a general trend that the region of strong coupling for TM diborides shifts down to lower energies as found for conventional superconductors thus leaving hope only for modest T_c 's. The existence of 2D- and 3D-type Fermi sheets derived mainly from boron σ and π bands, respectively, has been shown to be important for a quantitative understanding of the transport properties of MgB_2 [10]. The 2D Fermi surface is connected to the hole doping of boron $2p$ bands and does not seem to be important for transition metal diborides.

We have also calculated the relevant parameters for the description of the superconducting properties within the Eliashberg formalism. The results are compiled in Tab. III. A common feature unfavorable for superconductivity found in all transition metal diborides is the comparatively low ω_{log} . This quantity represents the effective average frequency of the coupling modes and sets

TABLE III: Average coupling constant λ , effective average phonon frequency ω_{log} (in meV), and estimates of T_c from the linearized gap equation. $N(0)$ denotes the density of states at the Fermi energy (per unit cell and spin).

	$N(0)$	λ	ω_{log}	T_c ($\mu^*=0.13$)
MgB_2	0.335	0.73	60.9	21.7
AlB_2	0.184	0.43	49.9	2.3
TaB_2	0.452	0.79	25.8	10.6
VB_2	0.592	0.28	44.1	< 1
NbB_2	0.520	0.67	30.5	8.4
TiB_2	0.179	0.10	52.9	-
YB_2	0.560	0.46	37.4	2.4

the energy scale for the pairing interaction. Its small value as compared to MgB_2 indicates that the pairing interaction is mainly mediated by the TM vibrations and not by the boron modes. The isotropic coupling constant λ shows a variation from weak to intermediate coupling strength. In Tab. III, we have also included values for the superconducting transition temperature as obtained by solving the linearized isotropic gap equations. The T_c values depend strongly on the screening properties expressed by μ^* and drop appreciably for $\mu^* > 0$. The values shown for a typical metallic screening of $\mu^* = 0.13$ thus should only be taken as indicators of the general trend. Furthermore, as mentioned before, for MgB_2 it is necessary to go beyond the isotropic limit and take into account the multigap structure introduced by the particular Fermi surface geometry for a proper quantitative description of the pairing state. Anisotropy is expected to play a minor role for the coupling in the low-frequency region of the transition metal vibrations that are dominated by the 3D-metal bands.

The values of λ and ω_{log} are most favorable for MgB_2 . The next promising candidates according to the present calculations are TaB_2 and NbB_2 , for which some authors find superconductivity at 9.5 K and 6.4 K, respectively [5]. Differences in stoichiometry might be able to explain different experimental results. As far as a comparison to recent point-contact measurements is possible we can state that the maxima in our $G(\omega)$ correspond well to the peaks found in the second derivative of the $I - V$ characteristic. There is also agreement in a strongly reduced electron-phonon coupling strength for transition metal diborides with respect to MgB_2 . We, however, want to mention that the reported very small numerical values for λ_{PC} should not be compared directly to our values since point contact experiments do not measure the McMillan λ .

To summarize, we have presented measurements of the generalized phonon density-of-states for various transition metal diborides. The observed trends in the lattice dynamics can be well ascribed by first principles calculations and do not exhibit indications of strong electron-phonon interaction. This view is supported by theoretical calculations of the electron-phonon coupling. While

they do not exclude the possibility of superconductivity with low T_c mediated by TM vibrations, they underline

the outstanding properties of MgB_2 among the class of diborides.

-
- [1] J. Kortus, I.I. Mazin, K.D. Belashchenko, V.P. Antropov, and L.L. Boyer, Phys. Rev. Lett. **86**, 4656 (2001).
 - [2] C. Buzea and T. Yamashita, Supercond. Sci. Technol. **14**, R115 (2001).
 - [3] P. Vajeeston, P. Ravindran, C. Ravi, and R. Asokamani, Phys. Rev. B **63**, 045115 (2001).
 - [4] Y. G. Naidyuk, O. E. Kvitnitskaya, I. K. Yanson, S.-L. Drechsler, G. Behr, and S. Otani, Phys. Rev. B, **66**, 140301 (2003).
 - [5] R. Heid, K.-P. Bohnen, and B. Renker, Adv. in Solid State Phys.**42**, 293 (2002).
 - [6] K.-P. Bohnen, R. Heid, and B. Renker, Phys. Rev. Lett. **86**, 5771 (2001).
 - [7] G. B. Bachelet, D. R. Haman, M. Schlüter, Phys. Rev. B **26**, 4199 (1982).
 - [8] K. M. Ho and K.-P. Bohnen, Phys. Rev. B **32**, 3446 (1985).
 - [9] D. Vanderbilt, Phys. Rev. B **32**, 8412 (1985).
 - [10] S. Tsuda, T. Yokoya, T. Kiss, Y. Takano, K. Togano, H. Kito, H. Ihara, and S. Shin, Phys. Rev. Lett. **87**, 177006 (2001).